

Effect of a Charge-Transfer Interaction on the Catalytic Activity of Acyl-CoA Dehydrogenase: A Theoretical Study of the Role of Oxidized Flavin

Olga Dmitrenko,* Colin Thorpe, and Robert D. Bach*

Department of Chemistry and Biochemistry, University of Delaware, Newark, Delaware 19716

Received: April 2, 2003; In Final Form: August 9, 2003

To examine the role of charge transfer (CT) interactions in the catalytic activity of acyl-CoA dehydrogenase, model systems for the reactant complex of tricyclic or bicyclic models of FAD (Fl_{ox}) with the thioenolate portion of acyl-CoA were studied. Singlet excitation energies have been estimated at the TD-B3LYP/6-31G(d)//B3LYP/6-31+G(d,p) level of theory. Location and intensity of the charge-transfer band in the UV-absorption spectrum of the thioenolate/ Fl_{ox} complex depends on the distance between model substrate and isoalloxazine ring and becomes prominent at approximately the van der Waals contact distance. The prereaction complex for hydride transfer from the thioenolate to flavin [fully optimized at B3LYP/6-31+G(d,p)] possesses a sandwich-like structure with a contact distance of about 3.7 Å between participants and has about 0.7 electrons transferred from the enolate to the flavin. We suggest that the formation of a CT complex in the enzyme has a significant impact on the barrier to α -proton abstraction; it reduces the α -proton affinity of the thioester, thereby lowering the activation energy for the first step in this enzymatic process.

1. Introduction

Acyl-CoA dehydrogenases catalyze the two-electron oxidation of a broad range of fatty acids with the conversion of acyl-CoA thioesters to their corresponding α , β -enoyl-CoA products. Dehydrogenation occurs by the breakage of two kinetically stable C—H bonds of the substrate, introducing a carbon—carbon double bond as shown in Scheme 1.¹ The first C—H bond breaking requires chemical activation of an adjacent thioester functionality and abstraction of hydrogen as a proton by the weakly basic Glu376-COO[−] with, what is presumed to be, a concomitant expulsion of a β -hydride that is transferred to N-5 of the FAD isoalloxazine ring.

Our recent computational study^{2a} has suggested that placement of a desolvated carboxylate base in the reaction cluster and the subsequent reapportionment of negative charge and ionic hydrogen-bonding interactions over all cluster species are a key feature of this enolization reaction. It was demonstrated computationally that H-bonds to the carbonyl oxygen of the incipient enolate significantly reduces the proton affinity of the α -proton and, consequently, decreases the pK_{a} . A linear relationship between PA and pK_{a} for carboxylic acids has been demonstrated computationally.^{2b} Thus, a reduction of the proton affinity provides a closer match of the pK_{a} 's, a decrease in the reaction endothermicity and consequently a lowering of the reaction barrier for α -proton abstraction.

Analysis of the X-ray structure of the medium-chain acyl-CoA dehydrogenase (MCAD)³ shown in Figure 1 has revealed the potential importance of a sandwich-like arrangement of the planes of substrate and isoalloxazine ring system of FAD with distances of 3.6 and 3.8 Å (C1C4a and C α C10a). A number of experimental studies have provided spectroscopic evidence for the formation of a charge-transfer complex between FAD and CoA analogues.⁴ Recently, Rudik and Thorpe raised the possibility that a charge-transfer (CT) interaction between the developing enolate and the flavin chromophore contributes to

SCHEME 1

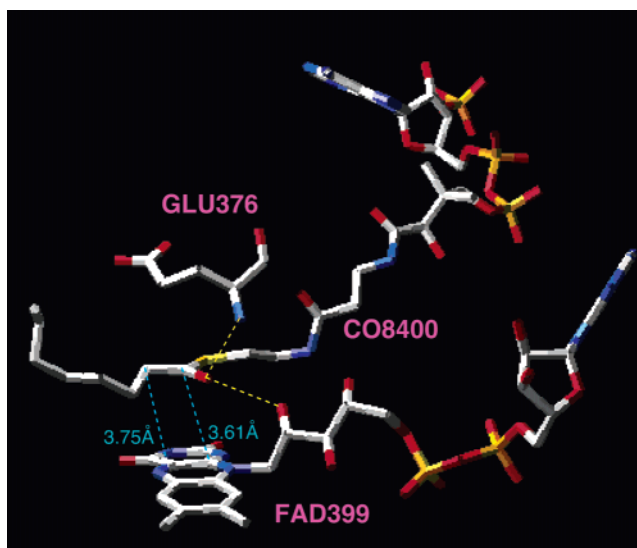
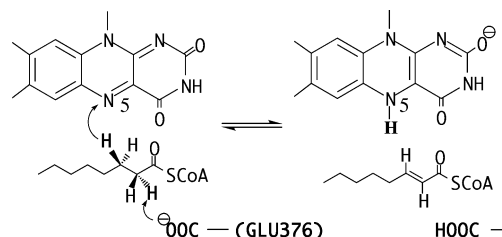


Figure 1. Octanoyl-CoA substrate and selected residues of the X-ray structure for medium-chain acyl-CoA dehydrogenase.³

the stabilization of the transition state during the dehydrogenation of CoA-thioester substrates.⁵

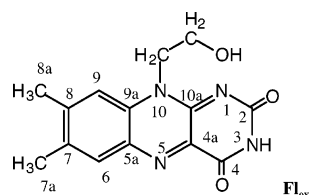
In this paper we address the influence of a CT interaction on the mechanism of α -proton abstraction without concern for the concomitant transfer of a hydride equivalent to the flavin. There

is unequivocal experimental evidence for uncoupling α -proton abstraction from reduction of the flavin ring using 3-substituted redox-inactive thioester analogues.^{1b,d,4} It is not our intent to represent the enzyme itself but rather to provide a model system that serves to describe the intrinsic gas-phase behavior to illustrate how the proximity of the tricyclic oxidized flavin (Fl_{ox}) affects the activation barrier for α -proton removal.

2. Computational Details

2.1. Methods. Quantum chemistry calculations were carried out using the Gaussian98 program system⁶ utilizing gradient geometry optimization.⁷ All geometries were fully optimized using the B3LYP functional^{8,9} with 6-31G(d) and 6-31+G(d,p) basis sets. Vibrational frequency calculations at the B3LYP/6-31G(d) level of theory were performed to characterize the stationary points as either minima or transition structures (first-order saddle point). Proton affinities (PA) were estimated as the difference in total energy between the protonated and the corresponding neutral species at the B3LYP/6-31+G(d,p) level of theory. It has been shown that such an estimation produces PA values that are systematically higher by 3–5 kcal/mol than experimental PA values.^{2a} Unless otherwise stated, all energy values quoted in the text are at the B3LYP/6-31+G(d,p) level. Vertical energies of the singlet excited-state transitions have been calculated using the time-dependent DFT method,¹⁰ TD B3LYP/6-31G(d). Corrections for solvation were made using polarizable conductor COSMO model calculations.¹¹

2.2. Models. The model systems in this study are designed on the basis of a fragment of the active site of the X-ray structure for medium-chain acyl-CoA dehydrogenase.³ Thioester $\text{CH}_3\text{-CH}_2\text{CH}_2(\text{C}=\text{O})\text{SCH}_3$ was chosen to represent the CoA substrate. It is well established that the weakly acidic α -proton of the CoA substrate is activated by two key hydrogen bonding interactions with the 2'-hydroxyl group of the ribityl side chain of FAD and a backbone N—H donor.^{1d,3a,b} The active site base ($-\text{COO}^-$) and the amide hydrogen donor ($\text{H}-\text{N}<$) are combined in a single molecule [$\text{H}(\text{C}=\text{O})-\text{NH}-\text{CH}_2\text{CH}_2\text{CH}_2\text{COO}^-$] that mimics the GLU376 side chain. To model FAD, we used a tricyclic oxidized flavin molecule (Fl_{ox}) with the 2'-OH group of the



ribityl moiety represented by a $-\text{CH}_2\text{CH}_2\text{OH}$ group that forms the second hydrogen bond to the substrate carbonyl oxygen. In some preliminary calculations, we used the smaller model compounds, bicyclic flavin (pterin derivative) and $\text{CH}_3\text{CH}_2(\text{C}=\text{O})\text{SCH}_3$.

3. Results and Discussion

3.1. Effect of Flavin Proximity on the α -Proton Affinity of the Thioester. In an earlier computational study we demonstrated the importance of hydrogen bonding to the carbonyl oxygen in lowering the barrier for α -proton abstraction.^{2a} Their major contribution to the catalysis is lowering the pK_a of the α -proton.² The effect of H-bond donors on the relative stability of the enolate ion resulting from α -proton abstraction can be predicted from their respective proton affinities (Table 1) estimated from B3LYP/6-31+G(d,p) total energies. Naked thioenolate anion, $[\text{CH}_3\text{CH}(\text{C}=\text{O})\text{SCH}_3]^-$, has a much higher

TABLE 1: Estimated Proton Affinities (PA) of Anionic Bases and Enolate Intermediates Based upon B3LYP/6-31+G(d,p) Total Energies^a

anion	PA (kcal/mol)
CH_3COO^-	352.9
$(\text{CHO})\text{NHCH}_2\text{CH}_2\text{CH}_2\text{COO}^-$ (all trans)	345.1
$\text{CH}_3\text{CH}(\text{C}=\text{O})\text{SCH}_3$	369.2
$\text{CH}_3\text{CH}_2\text{CH}(\text{C}=\text{O})\text{SCH}_3$	367.9
$\text{CH}_3\text{CH}(\text{C}=\text{O})\text{SCH}_3 \cdots \text{HNCH}_3(\text{C}=\text{O})\text{H}$	354.3
$\text{CH}_3\text{CH}(\text{C}=\text{O})\text{SCH}_3 \cdots (\text{CH}_3\text{OH}) \cdots \text{HNCH}_3(\text{C}=\text{O})\text{H}$	345.3
$\text{CH}_3\text{CH}_2\text{CH}(\text{C}=\text{O})\text{SCH}_3 \cdots \text{CH}_3\text{OH}$	359.1

^a Symbol “ \cdots ” denotes hydrogen bonding between the boldface hydrogen and carbonyl oxygen of the substrate.

PA than acetate anion (367.9 vs 352.9 kcal/mol), which means that, in the absence of some external influence, acetate anion is too weakly basic to abstract an α -proton from substrate thioester. For this reason, neither a transition structure nor a product cluster have been located during computational attempts to abstract the thioester α -proton with a carboxylate base.^{2a} Two H-donors to the model substrate reduce the α -proton affinity to the value 345.3 kcal/mol ($\Delta\text{PA} = 23.9$ kcal/mol), which is now 7.6 kcal/mol lower than the PA of the base, acetate anion (Table 1). The effect of just one H-donor, the N—H of methylformamide, is not as pronounced; the PA of acetate anion is slightly lower (by 1.4 kcal/mol) than the PA of the α -proton in thioenolate \cdots methylformamide complex $[\text{CH}_3\text{CH}(\text{C}=\text{O})\text{SCH}_3 \cdots \text{HNCH}_3(\text{C}=\text{O})\text{H}]$. This H-bond mediated reduction of the energy needed for α -proton abstraction from the thioester leads to a significant decrease [from 10.4 (one H-donor) to 5.8 kcal/mol (two H-donors)] in the reaction barrier (Scheme 2).

To get an initial idea how the flavin proximity to the CoA substrate observed in the X-ray structure of the active site may affect the α -proton abstraction, we estimated proton affinities for a simplified sandwich-like complex consisting of thioenolate, $\text{CH}_3\text{CH}(\text{C}=\text{O})\text{SCH}_3^-$, and a bicyclic oxidized flavin model (Figure 2). The contact distance (d , Å) between approximates planes of the two components was varied between 3.0 and 5.0 Å. The starting complexes, both neutral and anionic, were optimized at the B3LYP/6-31+G(d,p) level with the two C—C distances (see Figure 2) fixed to 3 Å and the two dihedral angles fixed to $\pm 90^\circ$ to keep the planes of the flavin model [defined by $\{\text{N}5, \text{C}4a, \text{C}10a\}$] and substrate [defined by $\{\text{O}=\text{C}1\alpha\}$] approximately parallel. For all other structures with d greater than 3 Å, the contact distance was gradually increased but no re-optimization was performed.

The results of this exercise (Figure 2) show that the proximity of the flavin to the substrate, within the van der Waals contact distance, may have a very strong acidifying effect upon the α -hydrogen of the thioester. In this simple model, the estimated reduction in PA is about 20 kcal/mol (corresponding to an acidification of about 4–5 pK_a units^{2b}), suggesting that bases even weaker than the acetate anion could, in principle, be effective in abstracting the α -proton.

3.2. α -Proton Abstraction from Thioester with and without Tricyclic Oxidized Flavin, Fl_{ox} . The model base $(\text{CHO})\text{-NHCH}_2\text{CH}_2\text{CH}_2\text{COO}^-$, which mimics GLU376, has an estimated $\text{PA} = 345.1$ kcal/mol (Table 1). To achieve α -proton abstraction with an acceptable activation barrier, it is essential to match the PA of the α -proton of the substrate to that of the base. Thus, comparing the PA value of the butanoic thioester, $\text{CH}_3\text{CH}_2\text{CH}(\text{C}=\text{O})\text{SCH}_3^-$, with the plot of proton affinities vs contact distance d (Å) given in Figure 2, suggests that the PA match can be achieved by docking a flavin molecule in close

SCHEME 2

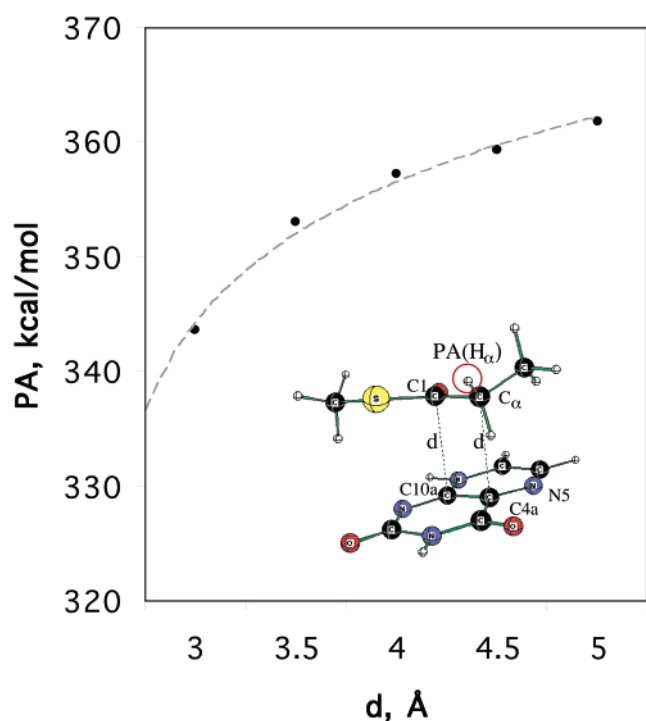
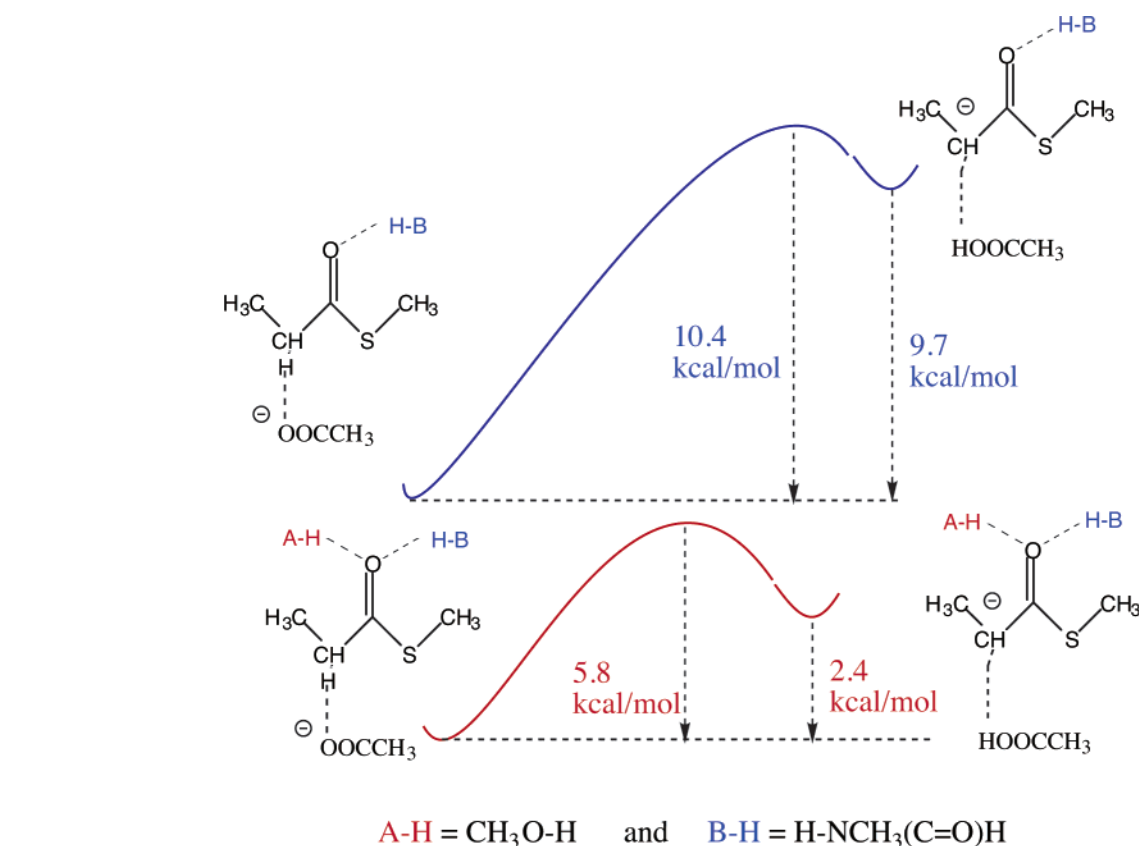


Figure 2. Dependence of α -proton affinity for the $\text{CH}_3\text{CH}(\text{C}=\text{O})\text{SCH}_3^-/\text{Fl}_{\text{ox}}$ model anionic complex (shown in insertion) on the contact distance to flavin (d , Å) estimated at the B3LYP/6-31+G(d,p) level of theory.

proximity to the thioester substrate. The PA of the model thioester α -proton is decreased about 20 kcal/mol when distance d between planes of the two components is decreased from 5 to 3 Å. Thus, a significant reduction of the reaction barrier when a flavin molecule is docked in a sandwich-like structure with the distance $d = 3$ Å (which is about the sum of van der Waals

radii of two carbons) compared to the case of model without flavin can be anticipated.

First, it is necessary to calculate the α -proton abstraction barrier in the absence of the flavin. The prereaction complex, transition structure, and product complex were optimized^{2a} for the model system without flavin (Figure 3). The reaction barrier for the α -proton abstraction is ca. 7.7 kcal/mol.

Then the tricyclic oxidized flavin molecule Fl_{ox} was placed with the orientation appropriate to the crystal structure of the enzyme. The prereaction complex, transition structure and product complex have been optimized with two C—C distances (C1—C10a and $\text{C}\alpha\text{—C4a}$) constrained to 3 Å. The resulting reaction barrier was found to be about 2-fold lower (3.6 kcal/mol, Figure 4) than the barrier for α -proton abstraction in model system $\text{CH}_3\text{CH}_2\text{CH}_2(\text{C}=\text{O})\text{SCH}_3$ without the stabilizing influence of the flavin, Fl_{ox} . Thus, the basic premise outlined in the Introduction has merit, and we suggest that the close proximity of the oxidized flavin to the CoA substrate suggested by the X-ray structure (3.61 and 3.75 Å, Figure 1) does play a role in lowering the activation barrier for α -proton abstraction. The developing negative charge on the thioenolate can be delocalized by the thiocarbonyl moiety as well as by charge transfer to the isoalloxazine system. This is consistent with the earlier results on the medium chain acyl-CoA dehydrogenase substituted with 5-deaza FAD.⁵

We also examined the effect of varying the distance d between the two parallel planes of the model reactants on the activation barrier. Similar calculations performed for the system with contact distance $d = 4$ Å, but with a smaller basis set (B3LYP/6-31G(d)) resulted in a reaction barrier 2.3 kcal/mol higher than that for the $d = 3$ Å at the same level of theory. However, this observation is confused by the fact that the 3 Å-constrained prereaction complex (Figure 4) is about 12 kcal/mol higher in energy than the 4 Å-constrained prereaction complex; the higher

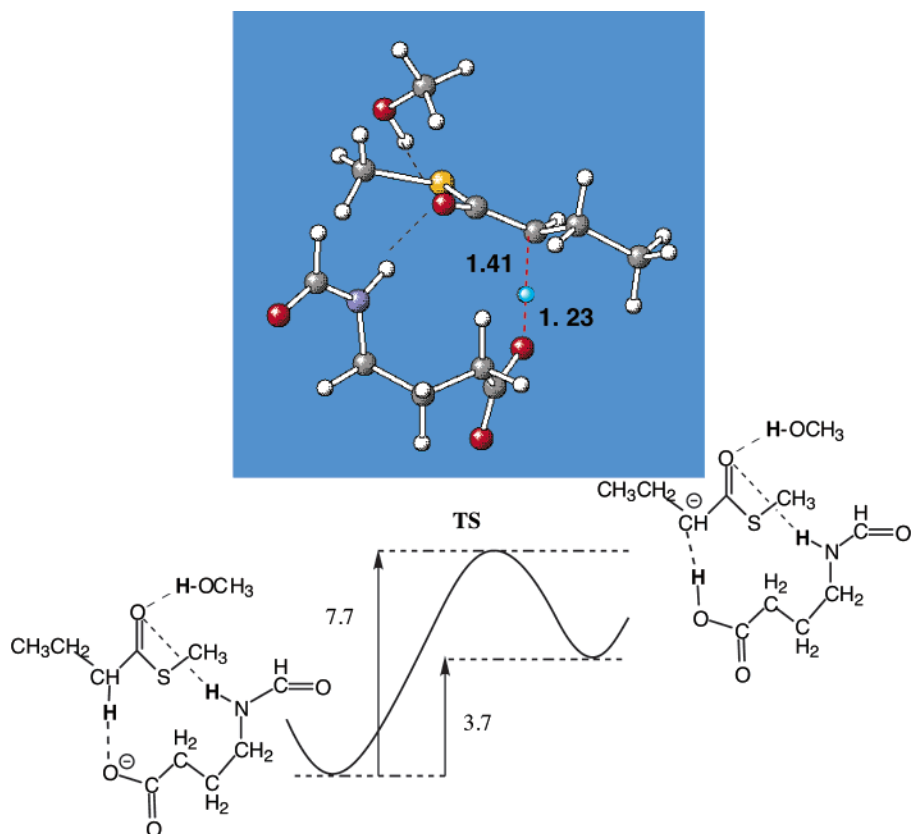


Figure 3. Fully optimized transition structure and relative energies (kcal/mol) of the prereaction cluster for the thioester, the TS, and the product cluster for the model system $\{\text{CH}_3\text{CH}_2\text{CHH}(\text{C}=\text{O})\text{SCH}_3 \cdot (\text{CH}_3\text{OH}, (\text{H}(\text{C}=\text{O})-\text{NH}-\text{CH}_2\text{CH}_2\text{CH}_2\text{COO}^\ominus))\}$ at the B3LYP/6-31+G(d,p) level of theory.

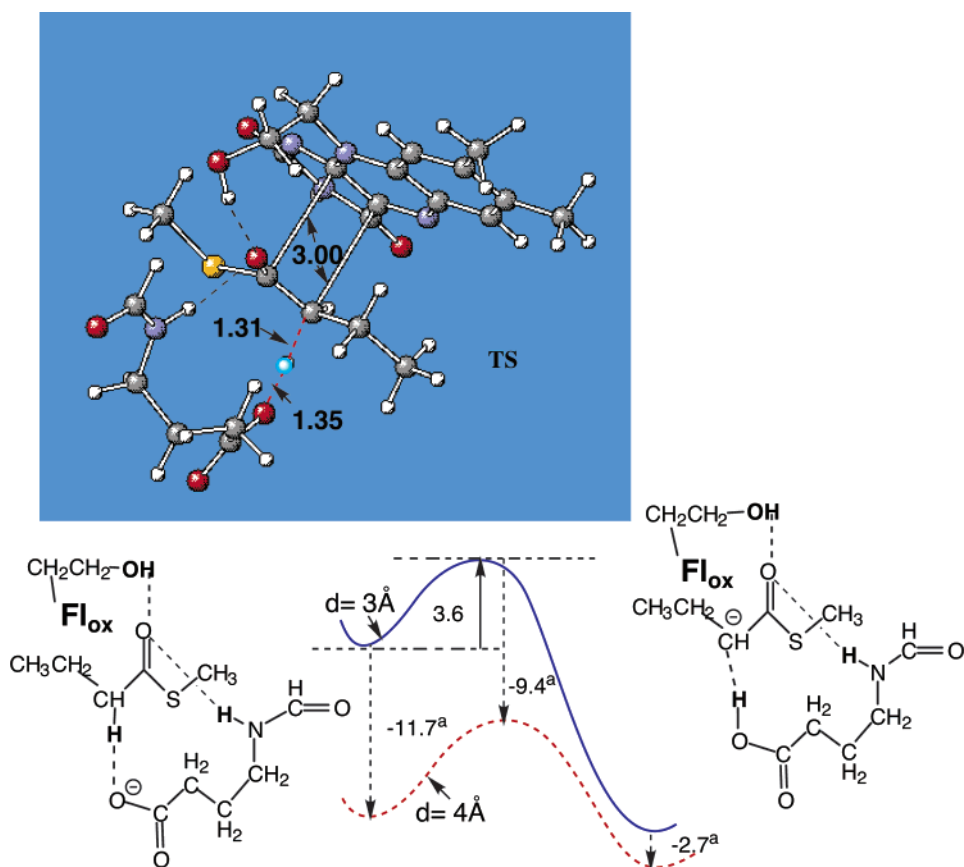


Figure 4. Transition structure optimized at the B3LYP/6-31+G(d,p) level for the α -proton abstraction reaction in the model system of acyl-CoA-dehydrogenase with docked oxidized flavin. The distance between Fl_{ox} and substrate is fixed to 3 Å. The reaction barrier and reaction energy (kcal/mol) are at the B3LYP/6-31+G(d,p) level of theory. The B3LYP/6-31G(d) energy differences (kcal/mol) for the prereaction complexes, TSs, and product complexes are calculated for two model systems with $d = 3$ Å (solid line) and $d = 4$ Å (dotted line).

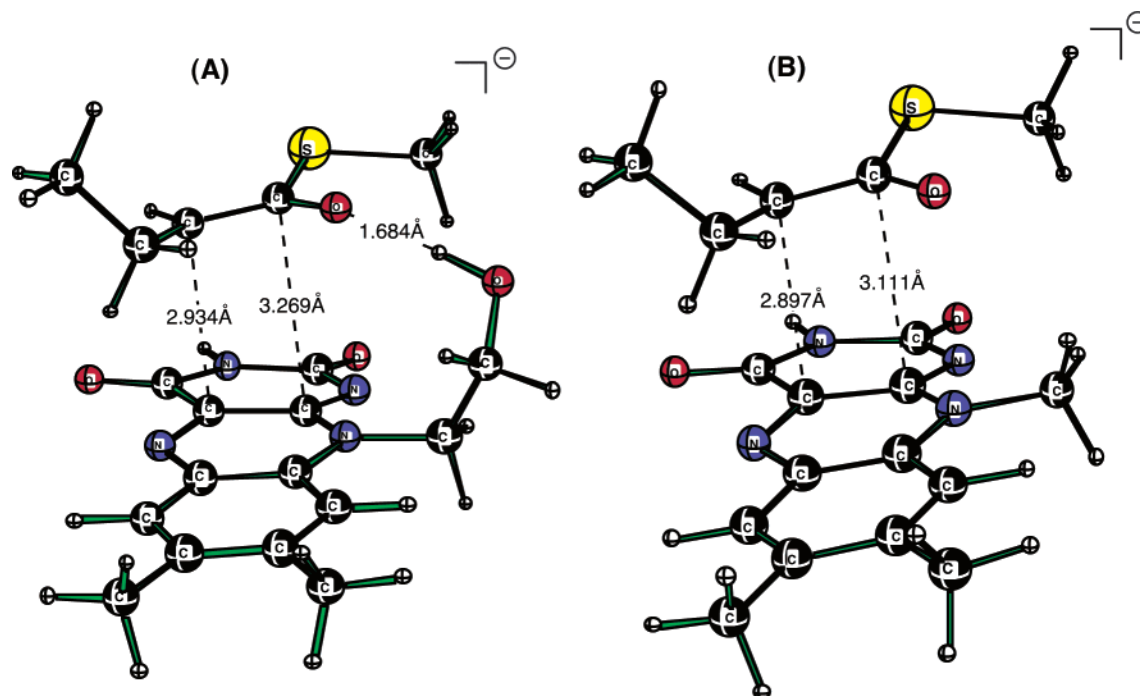
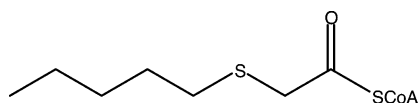


Figure 5. $\text{CH}_3\text{CH}_2\text{CH}(\text{C}=\text{O})\text{SCH}_3^-/\text{Fl}_{\text{ox}}$ (anionic form of the substrate/flavin) complexes with the ribityl moiety represented by $-\text{CH}_2\text{CH}_2\text{OH}$ (A) and CH_3 (B) groups optimized at the B3LYP/6-31+G(d,p) level of theory.

energy starting complex gives the lower activation barrier! Nonetheless, one may conclude that flavin proximity does lower the reaction barrier for α -proton abstraction and that bringing the two components closer together by 1 Å may result in the above 2.3 kcal/mol barrier decrease corresponding to an approximate 50-fold increase in the reaction rate. The question remains as to just how this proximity effect lowers the activation barrier for α -proton abstraction.

3.3. Charge-Transfer Thioenolate/ Fl_{ox} Complexes and Their Spectral Characteristics. The experimental observations^{1d,4,5} that a charge-transfer band accompanies the removal of an α -proton from a modified β -thio CoA substrate that cannot enter into the second stage hydride transfer to flavin provides a rationale for the rate increase we have found computationally. Spectroscopic studies of the acyl-CoA dehydrogenase model with the redox-inactive thioester analogue 3-thia-octanoyl-CoA have indicated the appearance of an intense charge-transfer band (centered at 800 nm) generated upon removal of the weakly acid α -proton.^{4,5}



We found that the anionic form of thioester substrate $\text{CH}_3\text{CH}_2\text{CH}_2(\text{C}=\text{O})\text{SCH}_3^-$ and oxidized flavin form a stable sandwich-like complex without geometrical constraints. The relevant C—C bond distances between the two components were found to be 2.93 and 3.27 Å (Figure 5A). The energy of complexation relative to isolated reactants is 22.2 kcal/mol. When the ribityl moiety in Fl_{ox} , represented by the N10 $-\text{CH}_2\text{CH}_2\text{OH}$ group, is substituted by CH_3 (lumiflavin) to prevent the contribution of the H-bond stabilization, the complexation energy drops to 16.3 kcal/mol, which we assign to the charge-transfer interaction energy. Despite the decrease in complexation energy, in the absence of the intramolecular H-bond, the interacting flavin and thioenolate come into closer

TABLE 2: TD (B3LYP)/6-31G(d) Vertical Strongly Allowed Singlet–Singlet ($S_0 \rightarrow S_N$) Transitions (nm) Calculated for the $\text{CH}_3\text{SCH}(\text{C}=\text{O})\text{SCH}_3^-/\text{Fl}_{\text{ox}}$ Complex Optimized at the B3LYP/6-31G(d) Level (Plain Numbers) and at the B3LYP/6-31+G(d,p) Level (Bold Numbers)^a

$S_0 \rightarrow S_N$	gas-phase ($\epsilon = 1$)	THF ($\epsilon = 7.6$)
$S_0 \rightarrow S_1$ (HOMO–LUMO)	957 (0.11) 859 (0.13)	838 (0.11)
$S_0 \rightarrow S_6$	408 (0.11) 402 (0.12)	407 (0.13)
$S_0 \rightarrow S_{10}$	337 (0.05) 326 (0.05)	327 (0.10)

^a Oscillator strengths are given in parentheses. S_0 and S_N ($N = 1, 6, 10$) correspond to the ground and excited (N) singlet state. Calculations for systems in an environment with a dielectric constant of 7.58 (tetrahydrofuran, THF) were performed with the COSMO solvent model.¹¹

contact ($\text{C1C10a} = 3.11$ Å, $\text{C}\alpha\text{C4a} = 2.90$ Å vs 3.27 and 2.93 Å, Figure 5B).

Interestingly, when the thioenolate is replaced by the 3-thia-butanoyl-CoA model enolate ($\text{CH}_3\text{SCH}(\text{C}=\text{O})\text{SCH}_3^-$, Figure 6), the complexation energy is reduced significantly (15.6 vs 22.2 kcal/mol, Figures 6 and 5A), and the distance between substrate and flavin is markedly increased ($\text{C1C10a} = 3.44$ Å, $\text{C}\alpha\text{C4a} = 3.20$ Å).

To estimate the extent of charge transfer and the agreement with experiment, we performed TD DFT (B3LYP) calculations on the charge-transfer model complex of Fl_{ox} with the $\text{CH}_3\text{SCH}(\text{C}=\text{O})\text{SCH}_3^-$ model anionic form of the substrate (Figure 6). This charge-transfer complex has three major absorption bands characterized by the calculated Franck–Condon (FC) transitions at 957, 408, and 337 nm [TD B3LYP/6-31G(d)/B3LYP/6-31+G(d,p), Table 2]. The first transition can be assigned to a charge-transfer band that is in reasonable agreement with the experimental system (≈ 800 nm) when considering the abbreviation of our model and the difference in environment. The two latter transitions belong to flavin as indicated by the summary of TD B3LYP calculations for the

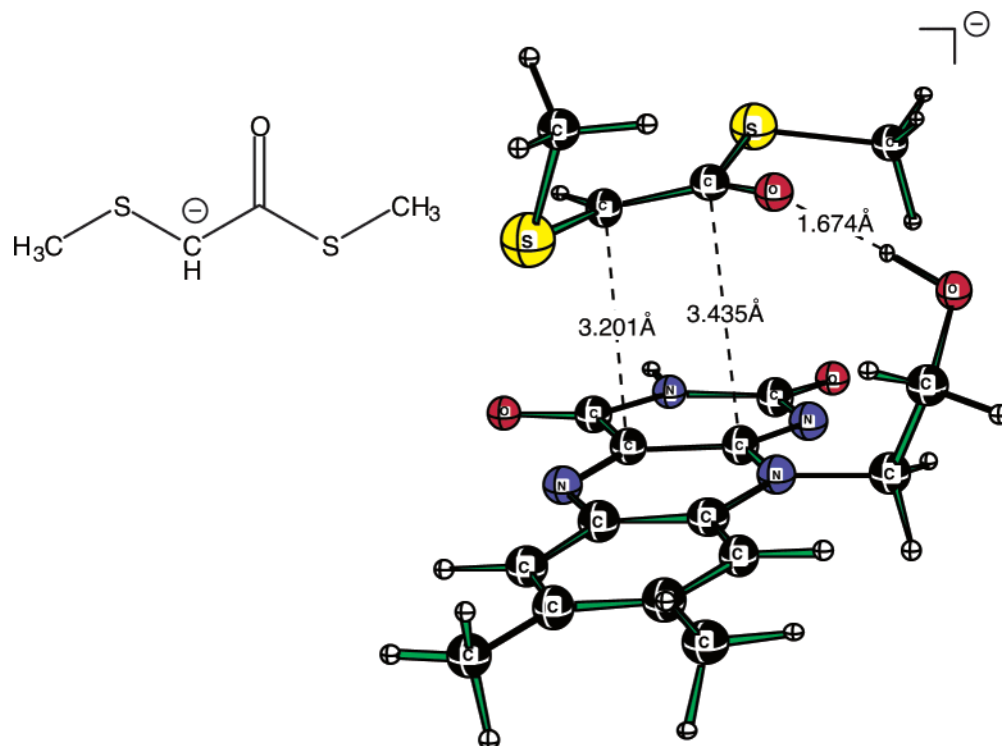


Figure 6. $\text{CH}_3\text{SCH}(\text{C}=\text{O})\text{SCH}_3^-/\text{Fl}_{\text{ox}}$ complex optimized at the B3LYP/6-31+G(d,p) level of theory. The total energy of complexation (including $\text{OH}\cdots\text{O}=\text{C}<$ bonding) is 15.6 kcal/mol.

TABLE 3: Low-Energy TD (B3LYP)/6-31G(d) Vertical Strongly Allowed Singlet–Singlet Transitions (nm) Calculated for Tricyclic Fl_{ox} Model with the Ribityl Moiety, Represented by the $-\text{CH}_2\text{CH}_2\text{OH}$ Group^a

transition	gas phase ($\epsilon = 1$)	THF ($\epsilon = 7.6$)	water ($\epsilon = 78.4$)
HOMO \rightarrow LUMO	410 (0.10) 411	410 (0.15)	413 (0.14)
HOMO–3 \rightarrow LUMO	341 (0.13) 342	337 (0.16)	345 (0.17)

^a Fl_{ox} was optimized at the B3LYP/6-31+G(d,p) level. Oscillator strengths are given in parentheses. Bold numbers correspond to TD B3LYP/6-31+G(d,p)/B3LYP/6-31+G(d,p) calculated transitions. Calculations for Fl_{ox} in an environment with a dielectric constant of 7.6 (tetrahydrofuran, THF) and of 78.4 (water) were performed with the COSMO solvent model.¹¹

flavin moiety itself (Table 3). We also examined the solvent effect (COSMO, Table 2) and found no significant changes except some increase in the oscillator strengths with the increase in dielectric constant. For a comparison, the absorption spectrum of lumiflavin in water shows two characteristic bands at 446 and 370 nm, followed by an intense band at 270 nm.¹² Thus, as also noted in ref 13, the theoretically predicted spectrum is somewhat (by about 30 nm) blue-shifted with respect to the experimental spectrum. It can be a result of specific media effect and a lack of model to account for a nonequilibrium solvation of the excited solute.

It should be noted that generally the TD DFT (B3LYP) approach predicts the excitation energies for low-lying excited states for single molecules remarkably well (very often within a few nm). As indicated in Table 2, the predicted CT band position is highly dependent upon the level of theory at which the complex has been optimized. The complex optimized with a smaller basis set [6-31G(d)] is tighter than the B3LYP/6-31+G(d,p) complex, and it has a shorter wavelength of the CT transition (859 nm). Thus, the dependence of the results on the basis set is due to the fact that the position of the CT band

is highly sensitive to the contact distance, which depends on flexibility of the basis set used in the optimization. Because we do not include in our model all the residues surrounding the substrate/ Fl_{ox} complex in studies of the acyl-CoA dehydrogenase with the redox-inactive thioester analogue 3-thiooctanoyl-CoA,⁵ one should not necessarily expect excellent agreement with experiment. The contact distance in the CT complex can be affected by external steric and electrostatic interactions or H-bondings that are not taken into account in the present models.

The LUMO orbital of flavin consists of bonding/antibonding interactions of π and π^* character: π (C8C7), π (C9C9a), lone-pair lp(N10), π^* (C4aN5), π^* (C10aN1), π^* (C2=O), and π^* (C4=O) orbitals (Figure 7).

The HOMO and HOMO–3 molecular orbitals are mostly different combinations of π orbitals (Figure 8). Interestingly, the π orbitals of the *ortho*-dimethylbenzene ring fragment are the most significant contributors to HOMO and HOMO–3, whereas LUMO employs orbitals of all three rings almost evenly.

The LUMO orbital of the oxidized flavin (Figure 8) exhibits the clearly distinguished π -character of the C4a–C10a bond. We suggest that this may result in a charge-transfer interaction (partial electron transfer) between the substrate and Fl_{ox} , in particular, if the substrate has a complementary developing π -bond with an excess of electrons.

In the $\text{CH}_3\text{SCH}(\text{C}=\text{O})\text{SCH}_3^-/\text{Fl}_{\text{ox}}$ model complex discussed above (Figure 6), the HOMO and LUMO orbitals responsible for generation of the CT band are the corresponding HOMO and LUMO of isolated participants, $\text{CH}_3\text{SCH}(\text{C}=\text{O})\text{SCH}_3^-$ and Fl_{ox} (Figure 9). The HOMO is composed largely of the high-lying thioenolate orbitals, and as anticipated, the LUMO orbital resides largely on the electron acceptor, the oxidized flavin moiety.

The same observation was made for $\text{CH}_3\text{CH}_2\text{CH}(\text{C}=\text{O})\text{SCH}_3^-/\text{Fl}_{\text{ox}}$ (anionic form of substrate/flavin) complexes that have been optimized with and without constraint of the C1C10a and

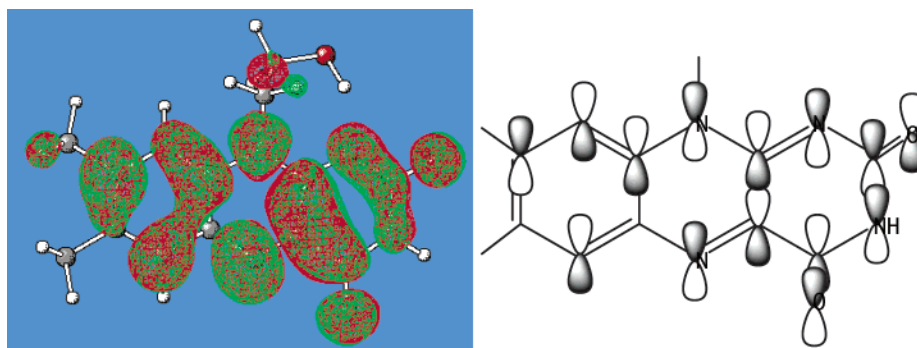
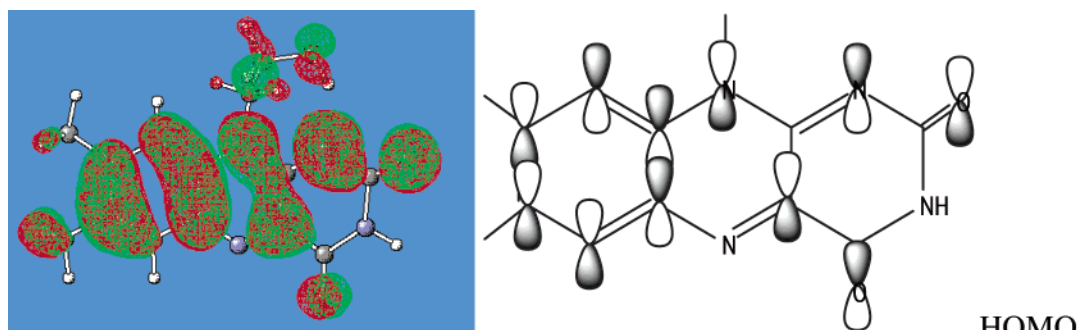
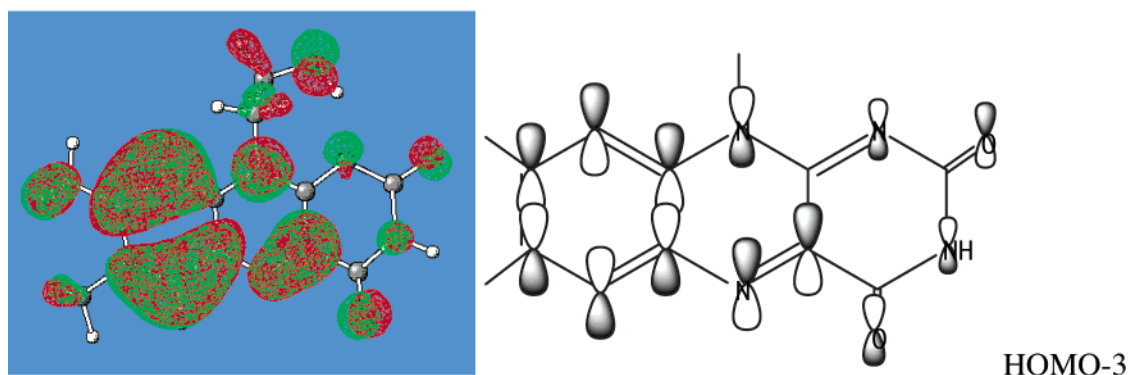


Figure 7. LUMO orbital of Fl_{ox} [B3LYP/6-31G(d)].



$\pi(\text{C6C7C8}), \pi(\text{C5aC9aC9}), \pi(\text{C4aN10}), \text{lp}(\text{N1}), \text{lp}(\text{O}_{\text{C2}}), \text{lp}(\text{O}_{\text{C4}})$



$\pi(\text{C7C6C5a}), \pi(\text{C8C9C9a}), \pi(\text{C4aN5}), \text{lp}(\text{N10}), \text{lp}(\text{O}_{\text{C4}}), \text{lp}(\text{O}_{\text{C2}}), \text{lp}(\text{N1}), \text{lp}(\text{N3})$

Figure 8. HOMO and (HOMO-3) orbitals of Fl_{ox} [B3LYP/6-31G(d)].

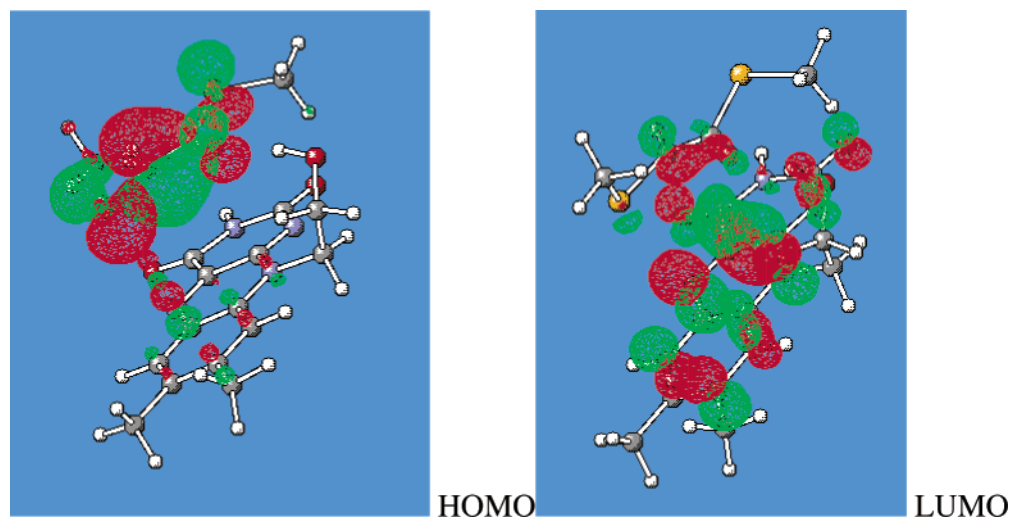


Figure 9. HOMO and LUMO orbitals for the $\text{CH}_3\text{SCH}(\text{C}=\text{O})\text{SCH}_3/\text{Fl}_{\text{ox}}$ complex (shown in Figure 6) responsible for the CT complex formation and its absorbance at the long-wavelength region.

TABLE 4: TD (B3LYP)/6-31G(d) Vertical Strongly Allowed Singlet–Singlet Transitions (nm) Calculated for the CH₃CH₂CH(C=O)SCH₃[−]/Fl_{ox} Complexes with Different Contact Distances: C1C10a=CαC10a = 3, 3.5, 4 Å^a

CT complex	3 Å	3.5 Å	4 Å
644, 647 (0.23)	645 (0.22)	961 (0.15)	1390 (0.10)
395, 400 (0.11)	392 (0.10)	410 (0.13)	418 (0.13)
321, 318 (0.05)	323 (0.04)	326 (0.08)	324 (0.08)
	Charge Transferred to Fl _{ox}		
−0.66	−0.61	−0.37	−0.33

^a The CT complex has been fully optimized at the B3LYP/6-31+G(d,p) level without geometrical constraint and is shown in Figure 5A. The estimated Mulliken charges (electrons) on Fl_{ox} are given in the last row. Bold numbers correspond to TD B3LYP/6-31+G(d,p)//B3LYP/6-31+G(d,p) calculations.

CαC4a distances. The CH₃CH₂CH(C=O)SCH₃[−]/Fl_{ox} complex optimized without constraints is shown in Figure 5A. Then, distances $d = \text{C1C10a} = \text{C}\alpha\text{C4a}$ were fixed to 3 Å, and the complex was re-optimized. Two other complexes with the $d = 3.5$ Å and $d = 4$ Å were taken for excited state energy calculations without further geometry optimization after the distance increase. The results summarized in Table 4 suggest that the CT band moves to the low-energy region and loses its intensity with an increase in contact distance d , whereas the two other flavin bands are not markedly affected. The decrease in contact distance leads to an increase in negative charge on Fl_{ox} up to about −0.7 e in the CT complex, which is 70% of the initial charge of “−1” initially provided by thioenolate anion.

4. Conclusions

The present computational study, in conjunction with available published experimental data on acyl-CoA-dehydrogenases, suggests that the developing enolate can be subjected to a strong charge-transfer interaction with flavin (16.3 kcal/mol). Analysis of the charge distribution in thioenolate/Fl_{ox} complexes indicates significant charge transfer to flavin (about 0.7 e). This type of complex is characterized by an intense charge-transfer absorption band (644 nm, gas phase) that is assigned to $\pi \rightarrow \pi^*$ transfer from the highest occupied molecular orbital of thioenolate to the lowest virtual orbital of flavin. The energy of this charge-transfer vertical (Franck–Condon) excitation depends strongly on the contact distance but appears less sensitive to the polarity of the microenvironment. Additional interactions, such as the aromatic stacking effects on the isoalloxazine ring described by Stankovich et al., may further modulate electronic distribution.¹⁴

The B3LYP calculations of two model systems (with and without flavin) designed for simulation of α -proton abstraction in acyl-CoA-dehydrogenases show that proximity of the flavin may have a strong impact on the reaction efficiency, leading to a 2-fold decrease in the reaction barrier. It is suggested that flavin proximity due to a charge-transfer interaction causes a significant acidifying effect on the substrate α -proton.

The available X-ray structures of acyl-CoA-dehydrogenases suggest that the geometrical constraint imposed by the active site of the enzyme as well as H-bonding with the substrate carbonyl oxygen forces the thioester substrate to reside within approximate van der Waals contact of the flavin prosthetic group. This, according to our computational simulations, should acidify the α -proton of the substrate and accelerate base-catalyzed proton abstraction. Thus, in addition to the reductive two-electron flavin chemistry¹⁵ involved in acyl-CoA-dehydrogenase function, our study suggests a catalytic role of the

oxidized flavin during α -proton abstraction. Similar charge-transfer role of the flavin has been suggested for an unusual flavoprotein, chorismate synthase. Our density functional calculations strongly support electron-transfer initiating phosphate elimination during turnover of the normal substrate to give an allylic radical intermediate.¹⁶

Acknowledgment. This work was supported by the National Science Foundation (CHE-0138632), by NIH GM26643, and partially by the National Computational Science Alliance under CHE990021N and utilized the NCSA SGI Origin2000 and University of Kentucky HP Superdome.

Supporting Information Available: Total energies and Cartesian coordinates of the optimized oxidized flavin, thioenolates and their complexes. This material is available free of charge via the Internet at <http://pubs.acs.org>

References and Notes

- (1) (a) Schopfer, L. M.; Massey, V.; Ghisla, S.; Thorpe, C. *Biochemistry* **1988**, 27, 6599. (b) Thorpe, C.; Kim, J.-J. P. *FASEB J.* **1995**, 9, 719. (c) Rudik, I.; Ghisla, S.; Thorpe, C. *Biochemistry* **1998**, 37, 8437. (d) Engst, S.; Vock, P.; Wang, M.; Kim, J.-J. P.; Ghisla, S. *Biochemistry* **1999**, 38, 257; and references therein. (e) Johnson, J. K.; Srivastava, D. K. *Biochemistry* **1993**, 32, 8004.
- (2) (a) Bach, R. D.; Thorpe, C.; Dmitrenko, O. J. *Phys. Chem. B* **2002**, 106 (16), 4325. (b) Peräkylä, M. *Phys. Chem. Chem. Phys.* **1999**, 1(24), 5643.
- (3) (a) Kim, J.-J. P.; Wang, M.; Paschke, R. *Proc. Natl. Acad. Sci. U.S.A.* **1993**, 90, 7523. (b) Djordjevic, S.; Pace, C. P.; Stankovich, M. T.; Kim, J. J. *Biochemistry* **1995**, 34, 2163. (c) PDB Ref. Code is 3MDE for medium-chain acyl-CoA dehydrogenase and 1BUC for butyryl-CoA dehydrogenase; Berman, H. M.; Westbrook, J.; Feng, Z.; Gilliland, G.; Bhat, T. N.; Weissig, H.; Shindyalov, I. N.; Bourne, P. E. *The Protein Data Bank. Nucleic Acids Research*, **2000**, 28, 235.
- (4) (a) Lau, S.-M.; Brantley, R. K.; Thorpe, C. *Biochemistry* **1988**, 27, 5089. (b) Tamaoki, H.; Nishina, Y.; Shiga, K.; Miura, R. *J. Biochem.* **1999**, 125, 285.
- (5) Rudik, I.; Thorpe, C. *Arch. Biochem. Biophys.* **2001**, 392 (2), 341.
- (6) Frisch, M. J.; Trucks, G. W.; Schlegel, H. B.; Scuseria, G. E.; Robb, M. A.; Cheeseman, J. R.; Zakrzewski, V. G.; Montgomery, J. A.; Stratmann, R. E.; Burant, J. C.; Dapprich, S.; Millam, J. M.; Daniels, A. D.; Kudin, K. N.; Strain, M. C.; Farkas, O.; Tomasi, J.; Barone, V.; Cossi, M.; Cammi, R.; Mennucci, B.; Pomelli, C.; Adamo, C.; Clifford, S.; Ochterski, J.; Petersson, G. A.; Ayala, P. Y.; Cui, Q.; Morokuma, K.; Malick, D. K.; Rabuck, A. D.; Raghavachari, K.; Foresman, J. B.; Cioslowski, J.; Ortiz, J. V.; Baboul, A. G.; Stefanov, B. B.; Liu, G.; Liashenko, A.; Piskorz, P.; Komaromi, I.; Gomperts, R.; Martin, R. L.; Fox, D. J.; Keith, T.; Al-Laham, M. A.; Peng, C. Y.; Nanayakkara, A.; Gonzalez, C.; Challacombe, M.; Gill, P. M. W.; Johnson, B.; Chen, W.; Wong, M. W.; Andres, J. L.; Gonzalez, C.; Head-Gordon, M.; Replogle, E. S.; Pople, J. A. *Gaussian 98, Revision A.7*, Gaussian, Inc., Pittsburgh, PA, 1998.
- (7) (a) Schlegel, H. B. *J. Comput. Chem.* **1982**, 3, 214. (b) Schlegel, H. B. *Adv. Chem. Phys.* **1987**, 67 (Pt. 1), 249. (c) Schlegel, H. B. In *Modern Electronic Structure Theory*; Yarkony, D. R., Ed.; World Scientific: Singapore, 1995; p 459.
- (8) (a) Becke, A. D. *Phys. Rev. A* **1988**, 38, 3098. (b) Lee, C.; Yang, W. and Parr, R. G. *Phys. Rev. B* **1988**, 37, 785.
- (9) (a) Becke, A. D. *J. Chem. Phys.* **1993**, 98, 5648. (b) Stevens, P. J.; Devlin, F. J.; Chabalowski, C. F. and Frisch, M. J. *J. Phys. Chem.* **1994**, 98, 11623.
- (10) (a) Bauernschmitt, R.; Ahlrichs, R. *Chem. Phys. Lett.* **1996**, 256, 454. (b) Casida, M. E.; Jamorski, C.; Casida, K. C.; Salahub, D. R. *J. Chem. Phys.* **1998**, 108, 4439. (c) Stratmann, R. E.; Scuseria, G. E.; Frisch, M. J. *J. Chem. Phys.* **1998**, 109, 8218.
- (11) Barone, V.; Cossi, M.; Tomasi, J. J. *Comput. Chem.* **1998**, 19, 404.
- (12) Dudley, K. H.; Ehrenberg, A.; Hemmerich, P.; Müller, F. *Helv. Chim. Acta* **1964**, 47, 1354.
- (13) Neiss, C.; Saalfrank, P.; Parac, M.; Grimme, S. *J. Phys. Chem. A* **2003**, 107 (1), 140.
- (14) (a) Pellett, J. D.; Sabaj, K. M.; Stephens, A. W.; Bell, A. F.; Wu, J. Q.; Tonge, P. J.; Stankovich, M. T. *Biochemistry* **2000**, 39 (45), 13982. (b) Pellett, J. D.; Becker, D. F.; Saenger, A. K.; Fuchs, J. A.; Stankovich, M. T. *Biochemistry* **2001**, 40 (25), 7720.
- (15) Bornemann, S. *Natural Prod. Reports* **2002**, 19 (6), 761.
- (16) Dmitrenko, O.; Wood, H. B.; Bach, R. D.; Ganem, B. *Org. Lett.* **2001**, 3 (26), 4137.